Parkinsonism and Related Disorders 132 (2025) 107318

Contents lists available at ScienceDirect

Parkinsonism and Related Disorders

journal homepage: www.elsevier.com/locate/parkreldis

Beyond the cerebello-thalamo-cortical tract: Remote structural changes after VIM-MRgFUS in essential tremor

Jonas Krauss [a,c,*], Neeraj Upadhyay [a], Veronika Purrer [b,c], Valeri Borger [d], Marcel Daamen [a], Angelika Maurer [a], Carsten Schmeel [e], Alexander Radbruch [b,e], Ullrich Wüllner [b,c,1], Henning Boecker [a,b,1]

[a] Clinical Functional Imaging Group, Department of Diagnostic and Interventional Radiology and Department of Nuclear Medicine, University Hospital Bonn, Bonn, Germany
[b] German Center for Neurodegenerative Diseases (DZNE) Bonn, Germany
[c] Department of Parkinson, Sleep and Movement Disorders, University Hospital Bonn, Germany
[d] Department of Neurosurgery, University Hospital Bonn, Germany
[e] Department of Neuroradiology, University Hospital Bonn, Germany

ARTICLE INFO

Keywords:
MRgFUS
Structural changes
VBM
VIM
Essential tremor

ABSTRACT

Introduction: Essential tremor (ET) is a progressive disorder characterized by altered network connectivity between the cerebellum, thalamus, and cortical regions. Magnetic Resonance-guided Focused Ultrasound (MRgFUS) of the ventral intermediate nucleus (VIM) is an effective, minimally invasive treatment for ET. The impact of MRgFUS interventions on regional Gray Matter Volume (GMV) are as yet not well understood.
Methods: Forty-six patients with medication-resistant ET underwent unilateral VIM-MRgFUS. Voxel-based morphometry was applied to investigate GMV changes over a time span of 6 months in the whole brain and the thalamus in particular to investigate local and distant effects.
Results: Clinically, contralateral tremor significantly decreased by 68 % at 6 months following MRgFUS. In addition to local GMV decreases in thalamic nuclei (VIM, ventral lateral posterior, centromedian thalamus and pulvinar), VBM revealed remote GMV decreases in the ipsilesional insula and the anterior cingulate cortex as well as the contralesional middle occipital gyrus. Increased GMV was found in the right superior and middle temporal gyrus, as well as in the left inferior temporal gyrus. There was no significant correlation between regional GMV declines and tremor improvement. However, temporal volume increases were associated with improved motor-related functional abilities and quality of life outcomes.
Conclusion: Our findings implicate distributed structural changes following unilateral VIM-MRgFUS. Structural losses could reflect Wallerian degeneration of VIM output neurons or plasticity due to decreased sensory input following tremor improvement.

1. Introduction

Essential tremor (ET) is a slowly progressive neurological disorder widely recognized as a network pathology. Despite extensive research, its pathophysiology remains incompletely understood. Neuroimaging studies using functional magnetic resonance imaging (fMRI) and positron emission tomography (PET) have highlighted alterations in functional connectivity within and between the cerebellum, thalamus, and various cortical motor regions as key contributors to ET pathogenesis [1]. Dysfunctions in aberrant cerebellar-thalamo-cortical loops are believed to play a pivotal role in the generation and propagation of tremor oscillations. Notably, the cerebellar dentate nucleus and the primary motor cortex (M1) are connected via the thalamic ventral intermediate nucleus (VIM) through the cerebello-thalamo-cortical tract (CTCT) which is implicated in ET pathophysiology [2].

Pharmacotherapy using β-blockers or primidone is the first-line

* Corresponding author. Clinical Functional Imaging Group, Department of Diagnostic and Interventional Radiology and Department of Nuclear Medicine, Department of Parkinson, Sleep and Movement Disorders, University Hospital Bonn, Germany Venusberg-Campus 1, 53127 Bonn, Germany.
E-mail address: jonas.krauss@ukbonn.de (J. Krauss).
[1] These authors share last authorship.

https://doi.org/10.1016/j.parkreldis.2025.107318
Received 10 November 2024; Received in revised form 24 January 2025; Accepted 1 February 2025
Available online 3 February 2025

therapy, but effectively controls symptoms in only approximately 50 % of patients and may lead to intolerable side effects for many patients [1]. As an alternative, stereotactic treatments have become well-established in recent years. Deep brain stimulation (DBS) is the most common surgical intervention, involving unilateral or bilateral implantation of electrodes in key areas of the pathological network (for ET, typically: VIM) to modulate aberrant neural activity via electrical currents. In addition to DBS, Magnetic Resonance-guided Focused Ultrasound (MRgFUS) offers an incisionless procedure that may surpass other thalamotomy procedures such as radio-surgical gamma knife [1]. Long-term treatment success has been demonstrated [3] but the adaptive processes associated with MRgFUS lesioning, need further investigation.

Using probabilistic tractography, we previously [4] reported significant reductions in streamline counts within the CTCT and a decrease in excitatory input from the VIM to the ipsilateral M1 following VIM MRgFUS treatment in ET patients. These findings align with a recent study [5], which described functional reorganization within the CTCT network encompassing M1, but also extending beyond, to dorsal attention (anterior cingulate cortex, superior temporal gyrus), and visual areas.

While numerous studies have documented functional changes within ET-related networks following VIM-MRgFUS [3,4], studies on subsequent gray matter volume (GMV) adaptations remain sparse, particularly at the whole-brain level: Observational patient studies have linked GMV alterations to motor and non-motor symptoms in both PD [6] and ET [7], while treatment studies in ET focusing on DBS have investigated morphological changes primarily in brain areas connected via the CTCT [8]. Meanwhile, changes may extend beyond the CTCT: for example, GMV changes in occipital areas associated with tremor reduction have been described in PD patients following VIM-MRgFUS treatment [9]. The structural reorganization upon MRgFUS in ET is as yet, however, unexplored. Remote network changes might explain further facets of clinical outcome after MRgFUS.

In this study we analyzed GMV changes at the whole-brain level using voxel-based morphometry (VBM), along with region-of-interest (ROI) analysis of thalamic subnuclei to further elucidate MRgFUS-related local structural adaptation. We hypothesized GMV decreases in brain structures linked directly via the CTCT, but also explored remote areas anatomically connected to the lesion center.

2. Methods

2.1. Patients

Fifty-two patients with diagnosis of definitive drug-refractory ET were recruited from the University Hospital Bonn, Germany. All patients underwent unilateral VIM-MRgFUS (ExAblate Neuro 4000, Insightec) between 2018 and 2023. Tremor presented bilaterally in every patient. Treatment targeted either the more affected hand or the dominant hand. Inclusion criteria are listed in the German Clinical Trials Registry (DRKS00016695). Apart from MRI-specific factors (e.g., claustrophobia, implanted electric devices, etc.), further exclusions criteria were brain scan irregularities, and comorbid psychiatric or neurological conditions. After excluding six patients due to poor image quality, the final sample included 46 patients (12 female, age: 73.48 ± 7.46 (mean ± standard deviation) characteristics Table 1.

The study was approved by the local ethics board of the University Hospital Bonn (No. 314/18), with informed consent obtained in accordance with the Declaration of Helsinki.

2.2. Study design

In this pre-post study design, MRI examinations were performed two days before the MRgFUS procedure, 3 days post, and 6 months post procedure. Additionally, clinical scales were administered to monitor patient-related outcomes of the MRgFUS procedure.

Table 1
Patient demographics.

Characteristics (n = 46)	Mean	Standard Deviation
Age	73.48	7.46
Sex: Male/female	34/12	–
Handedness: Right/non-right-handed	36/10	–
Age of onset	44.42	20.60
Disease duration	29.07	16.46
Alcohol sensitivity (%)	82 %	–
Presence of resting tremor	10	–
Treatment location VIM: Left/Right	39/7	–

2.3. Clinical assessment

To measure long-term clinical outcome, tremor assessments using the Fahn-Tolosa-Marin Clinical Rating Scale for Tremor (FTM) [10] before and 6 months after MRgFUS were compared, for the treated and untreated side separately. For this analysis, only upper extremity scores were included. Higher FTM scores indicate a more severe tremor presentation. The FTM comprises three parts: Part A + B which assess tremor severity and was summed up as FTM-A/B for the analysis and Part C which examines the impairments in activities of daily living (ADL).

Additionally, subjects completed the 36-Item Short Form Survey Instrument [11] (SF-36), a questionnaire measuring eight dimensions of health-related quality of life (QoL). Higher scores indicate better QoL per domain. Both tests are further described in Supplementary Table 3.

2.4. MRgFUS procedure

Details of the MRgFUS procedure were described previously [4]. Briefly, before MRgFUS, a clinical CT was performed to assess contraindications and confirm a skull density ratio of $\geq$0.3. For all but the first three patients, lesion site planning utilized preoperative probabilistic tractography from diffusion tensor imaging to map sensorimotor pathways (e.g., corticospinal tract, DRT, medial lemniscus). Standard VIM stereotactic coordinates were set at 14 mm lateral to the midline or 11 mm lateral to the third ventricle wall, and 25 % anterior to the posterior commissure along the intercommissural line. Adjustments were made intraoperatively based on subthreshold sonications (<50 °C), clinical tremor reduction, side effects, and pre-treatment DTI mapping. An average of 3.7 (±0.6) final sonications (>55 °C) were delivered to achieve optimal tremor reduction without adverse effects. Additional MRgFUS characteristics are detailed in Supplementary Table 1.

2.5. MRI data acquisition

All study participants underwent brain imaging with a 3T MRI scanner (Achieva TX, Philips Healthcare, Best, The Netherlands) equipped with an 8-channel head coil 2 days before, 3 days after, and 6-months after MRgFUS. A T1-weighted three-dimensional magnetization-prepared rapid gradient-echo (MPRAGE) sequence was acquired to obtain high-quality isotropic anatomical images. The following scanning parameters were used: 3D-FFE sequence; matrix size: 256 × 256 mm; TE/TR: 3.9/7.3 ms; flip angle: 15°; spatial resolution (acquired voxel size): 1 × 1 × 1 mm^3 with 0 mm interslice gap over 180 slices; scan duration: 4:40 min.

2.6. Manual lesion segmentation

Lesion segmentation was in accordance with previously reported procedures [12]. In native space, the lesion was segmented using FSLeyes (Version 0.34.2). In case the lesion was not well visible in a

patient, the SWI image was coregistered to the T1w image to enhance the accuracy of the lesion outline estimation. The maps were then nonlinearly normalized to the 1.5 mm voxel-size MNI152NLin2009cAsym template (Montreal Neurological Institute, Montreal, Canada) using Advanced Normalization Tools (ANTs, Philadelphia, PA, Version 2.3.1). For each follow-up, normalized lesion maps were summed up to identify areas with highest lesion/edema overlap among patients at the given timepoint. Finally, lesion volumes of the T1w images 3 days and 6 months after MRgFUS were calculated using the *fslstats* function.

2.7. Image preprocessing and voxel-based morphometry (VBM)

VBM analysis compared images acquired at baseline and 6 months following MRgFUS. After converting the DICOM image series to Nifti format, they were visually checked for artifacts and the origin manually set to the anterior commissure. Images of 7 patients operated on the right VIM were flipped using the *swapdim* command in FSL (FSL6.0.4, http://www.fmrib.ox.ac.uk/fsl). VBM was conducted using the longitudinal pipeline of the Computational Anatomy Toolbox 12 (CAT12.8.2, University Hospital Jena, Jena, Germany) [13] for Statistical Parametric Mapping 12 (SPM12, Wellcome Department of Cognitive Neurology, London, UK). SPM12 and CAT12 were running in MATLAB R2022a (The MathWorks Inc., Natick, MA, USA). Preprocessing involved segmenting the images into gray matter (GM), white matter, and cerebrospinal fluid probability maps. Tissue segmentations were registered to the MNI152NLin2009cAsym template using Diffeomorphic Anatomical Registration Through Exponentiated Lie algebra (DARTEL), with voxel size set to 1.5 mm. GMV segmentations underwent visual inspection, followed by quality control using CAT12s built-in function, with scans exceeding a z-score of 1.0 excluded. Finally, GMV maps were smoothed using a 6 mm full width, half maximum isotropic Gaussian kernel.

2.8. Statistical method

Assumption testing and inferential statistical analysis of the demographic and clinical data was conducted with SPSS (Version 27, IBM Corp., 2020). Outliers were checked, and normality was confirmed by visually inspecting QQ-plots. Pairwise *t*-tests were used to assess differences between the two time points.

For statistical voxel-wise comparison of the MRIs at whole-brain level, a pairwise *t*-test (Baseline (BL) vs 6-month post (6m)) was conducted using SPM12. The clusters were obtained at voxel-wise $p < 0.001$ and further corrected for multiple comparisons using cluster-level family-wise-error correction ($p < 0.05$ FWEc) according to Gaussian Random Field theory. Clusters were labeled according to the Automated Anatomical Labeling atlas version 3 (AAL3) [14].

Based on the lesion segmentation results, we further characterized the local thalamic effects of MRgFUS by a ROI-analysis, using the CAT12 preinstalled thalamic nuclei atlas by Saranthan et al. (2021) [15] that parcellates the thalamus in 12 nuclei per hemisphere. To adequately correct for multiple comparisons, we applied a Bonferroni-Holm correction using $p = 0.05$.

To investigate associations between GMV changes and clinical outcomes, mean beta values from significant clusters were correlated with tremor severity (FTM-A/B) and quality of life (QoL) measures (FTM-C, SF-36 subscores) using Pearson correlation coefficients. Change scores for these analyses were calculated as the difference between the 6-month and baseline measurements. Additionally, demographic variables (e.g., age, disease duration) were explored for associations with clinical outcomes and morphometric changes using Spearman correlation.

Furthermore, lesion volumes at 3 days and 6 months post-MRgFUS were correlated with aforementioned beta values and 6-month clinical outcomes using Pearson and Spearman correlation.

These analyses were exploratory in nature and were not corrected for multiple comparisons.

3. Results

3.1. Clinical outcomes

The FTM tremor scores decreased significantly ($t(45) = 15.71$, $p < 0.001$) from BL ($M = 19.51$, $SD = 5.20$) to 6m post-MRgFUS ($M = 6.28$, $SD = 4.86$) contralateral to the treated VIM, which reflects a mean improvement of ~70 %. The non-treated side did not show a significant difference ($t(45) = 0.63$, $p = 0.531$) from BL ($M = 17.47$, $SD = 6.10$)) to 6m ($M = 17.14$, $SD = 6.38$) (see Fig. 1).

ADL parameter (FTM part C) significantly improved by 66 % ($t(45) = 14.52$, $p < 0.001$) from BL ($M = 15.76$, $SD = 4.11$) to 6m ($M = 5.38$, $SD = 4.66$).

Comparing the scores at BL to 6m of the SF-36, the following QoL domains showed significant improvement: Physical and Emotional Role Functioning, Emotional Wellbeing, Social Functioning and General Health. Detailed statistics on clinical scores can be found in Supplementary Table 2.

3.2. Lesion segmentation

Lesion and edema regions were segmented for all included patients at 3 days post-procedure (shown in red/yellow in Fig. 2f) as well as in 34 patients 6 months-post procedure (shown in blue in Fig. 2f–g). Edema is known to increase in size shortly after MRgFUS [12], gradually shrinking as recovery progresses. This suggests that the actual lesion is concentrated around the center of mass seen in the 3-day post-procedure heatmap (yellow, Fig. 2f), which primarily aligns with the VIM area. The overlap of this lesion and edema region extends into adjacent areas, including the pulvinar (PV), centromedian (CM), and posterior ventrolateral thalamus (VLp).

Six months after procedure, the size of the hypointensities visible in the MPRAGE substantially decreased from 308.1 (±117.0) mm^3 to 22.8 (±17.3) mm^3 which is in line with what is usually reported in the literature [12]. The final lesion area was localized to the VIM area, but still reached the VLp and CM (Fig. 2 d, e, g). Fig. 2 provides a detailed illustration of this process and its outcomes.

3.3. VBM analysis

Structural changes from BL to 6m following VIM-MRgFUS revealed both local and remote alterations in GMV.

Consistent with the visual impression in the manual segmentation, a thalamic cluster with significant GMV decrease was observed which extended beyond the VIM (Fig. 3).

To further differentiate the affected thalamic nuclei, we conducted the follow-up atlas-based ROI-analysis: This confirmed a GMV decline in the target location (VIM) but also significant GMV reductions in the VLp and the CM, but also in the PV. Refer to Fig. 4 for visual representation of these results.

Additionally, GMV decline was detected in left insula, Rolandic operculum, left anterior cingulate cortex (ACC), and right middle occipital gyrus. Conversely, increases in GMV were observed in the right superior and middle temporal gyrus, as well as in the left inferior temporal gyrus (Fig. 3).

With a more lenient threshold ($p = 0.001$, uncorrected), additional trends to decreases at peak-level were found in the left middle occipital gyrus, the right temporal gyrus as well as the right cerebellar lobule VIII. See Supplementary Tables 4 and 5 for the statistics of each GMV decrease and increase at cluster-level comparing baseline and 6 month post treatment.

3.4. Correlation with clinical data

To assess associations between structural changes and clinical scores, we correlated the mean beta values from each significant cluster of the

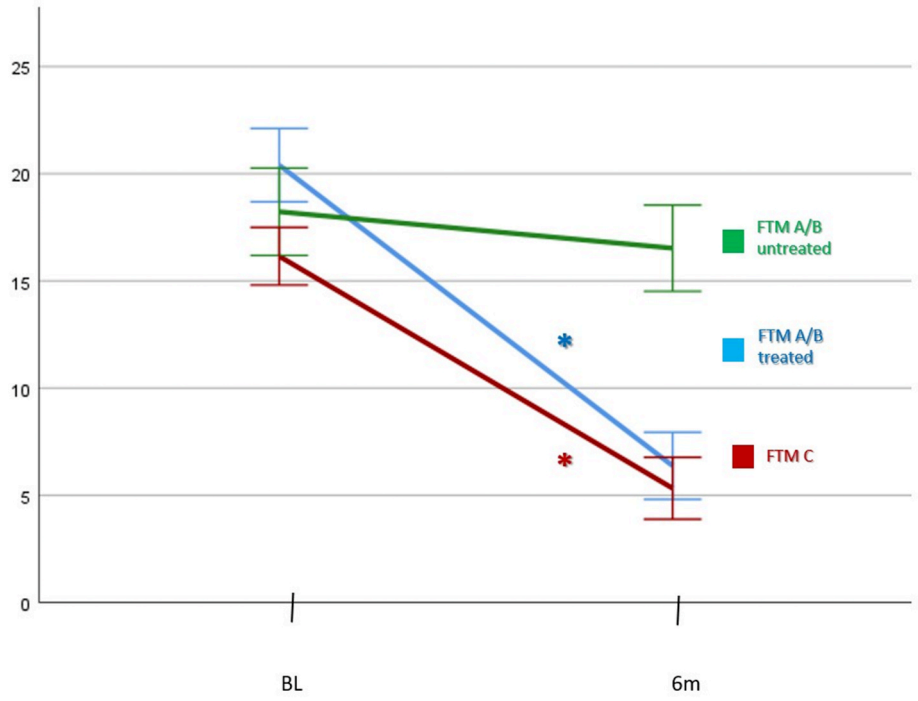

Fig. 1. FTM changes T0 versus 6 month post MRgFUS
Figure legend. FTM scores from T0 compared to 6 months following VIM-MRgFUS. Significant changes are visualized with an asterisk (*). The error bars represent standard deviations. Subscore of FTM-A and FTM-B were summed (FTM A/B) to indicate general tremor severity. (For interpretation of the references to colour in this figure legend, the reader is referred to the Web version of this article.).

voxel-wise analysis with FTM-A/B (tremor severity) as well as FTM-C (ADL), and the SF-36 subscales (indicating changes in QoL domains).

The reductions of the FTM-C showed a significant inverse correlation with GMV increase in the left inferior temporal gyrus ($r = -0.434$, $p = 0.007$). In addition, improvement in the SF-36 domain Physical Role Limitation ($r = 0.447$, $p = 0.015$) and Physical Functioning ($r = 0.368$, $p = 0.050$) showed correlations with GMV increase in right middle temporal gyrus.

Emotional Wellbeing was associated with GMV increase in the right middle temporal lobe ($r = 0.506$, $p = 0.005$). Moreover, there was a positive correlation between Social Functioning ($r = 0.380$, $p = 0.042$) and left middle temporal lobe increase as well as between improvement in General Health and left middle temporal lobe increase ($r = 0.537$, $p = 0.003$).

3.5. Correlation with demographics

Disease duration negatively correlated with GMV increases in the right middle temporal gyrus ($r = -0.369$, $p = 0.015$) and the left inferior temporal gyrus ($r = -0.337$, $p = 0.027$). No other significant correlations were found between demographic variables, morphometric changes, or clinical outcomes.

3.6. Correlation to lesion size

At 6 months, lesion size was positively correlated with GMV decrease in the ACC ($r = 0.358$, $p = 0.039$) and GMV increase in the right superior temporal gyrus ($r = 0.399$, $p = 0.024$). Lesion sizes at both 6m ($r = -0.437$, $p = 0.014$) and 3d ($r = -0.312$, $p = 0.034$) were associated with less pronounced GMV decline in the right middle occipital lobe. Additionally, lesion size at 3d correlated with GMV increases in the left inferior temporal gyrus ($r = 0.433$, $p = 0.005$) and showed a trend-level association with improved functional disability (FTM-C; $r = -0.283$, $p = 0.058$).

4. Discussion

Our study revealed significant GMV changes following the MRgFUS procedure targeting the VIM and induced substantial contralateral tremor reduction. We observed the expected GMV decrease in the VIM, but also in the adjacent VLp, CM, and PV. Additionally, remote GMV decreases were noted in the ipsilateral insula, the ipsilateral ACC, and the contralesional middle occipital gyrus (as well as, at trend level, in the ipsilesional middle occipital gyrus). On the other hand, we found increases in GMV in bilateral temporal gyri. Findings suggest distributed volumetric changes post-treatment, reflecting both direct effects of local ablation and broader network-level structural adaptations. While tremor improvement did not correlate with thalamic GMV decrease, improvements of functional disabilities, emotional well-being, social functioning and general health were significantly correlated with GMV increases in bilateral temporal areas.

At three days post-MRgFUS, MR images showed signal alterations extending beyond the ablation target (VIM), reflecting both the lesion and surrounding edema (Fig. 2a–b). Group-level density maps of these alterations (Fig. 2f) revealed the involvement of the VIM and surrounding nuclei (VLp, CM, PV). At six months, focal signal alterations were visible in about 75 % of patients (Fig. 2g), with segmentation overlap still extending beyond the VIM to include the VLp and CM. Statistical VBM analysis confirmed GMV decreases in the VIM, VLp, and CM, while also detecting PV changes. Findings highlight that MRgFUS primarily affects the VIM but also impacts adjacent thalamic nuclei. The lack of visible lesions in the PV at six months (Fig. 2g) alongside significant VBM changes (Fig. 3) suggests subtle structural changes, possibly triggered by initial edema and also inflammatory responses [16].

Whole-brain analysis at six months also indicates remote structural alterations (GMV decreases and increases) after the thalamic MRgFUS intervention, suggesting that lesion-induced changes extend to distant, yet connected cortical regions. As commonly seen in stroke patients, GMV changes can be caused by deafferentation of remote brain

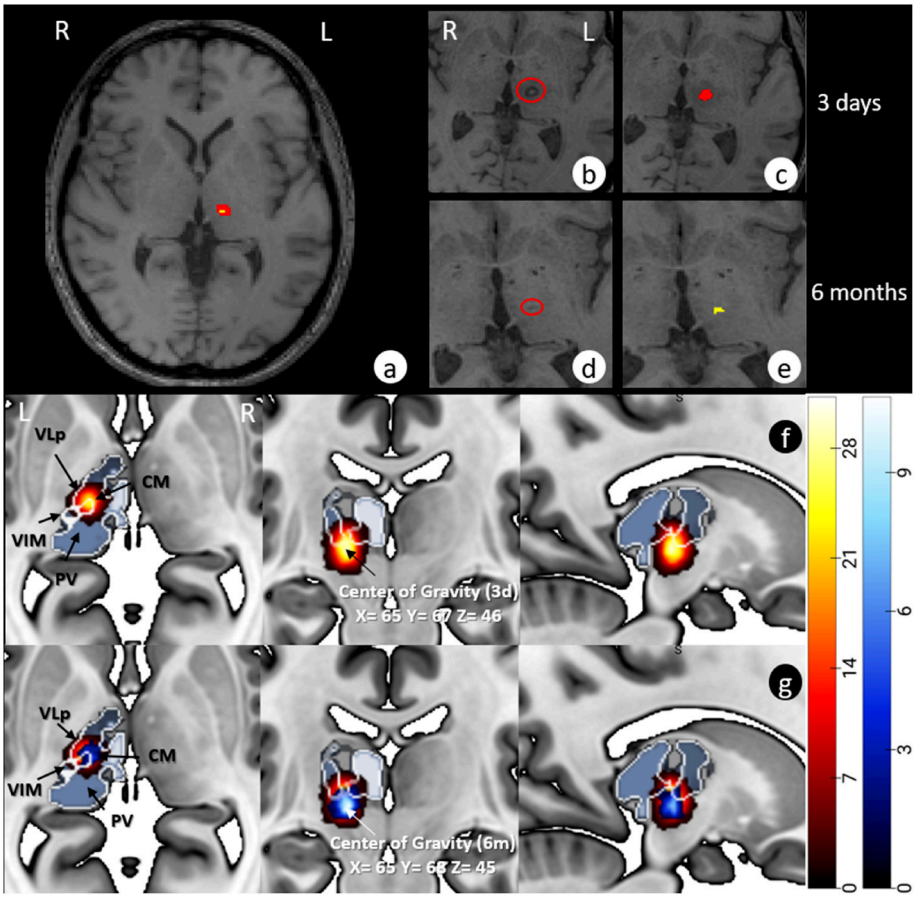

Fig. 2. Lesion segmentation workflow and overlap of 3 days and 6 months following MRgFUS
Figure legend. (a) Lesion overlap in MNI-space showing volume reduction from 3 days (3d) to 6 months (6m). (b–c) Lesion and edema 3 days post-treatment. (d–e) Same at 6m, showing edema recession. (f–g) Combined lesion masks 3d (red/yellow) and 6m (blue/white). (For interpretation of the references to colour in this figure legend, the reader is referred to the Web version of this article.)

structures connected with a lesion site. This process, known as Wallerian degeneration, has also been proposed as an underlying mechanism in the MRgFUS literature [17]. We observed a GMV decrease in the ipsilateral insula and ACC. While a precise map of thalamic subnuclei connections to the insula and ACC in humans has not yet been established, the thalamus, insula, and ACC are known to be structurally connected and form networks associated with a range of sensory and cognitive functions [18].

Regarding the insula, non-human primate studies using anterograde and retrograde tracing have highlighted connections of thalamic nuclei, located ventrally and within the intralaminar group (e.g., CM) and the PV [19]. Correspondingly, DTI analyses in humans demonstrated that the intralaminar group and specifically the medially located nuclei (e.g., CM) are connected to various cortical structures including the insula, suggesting involvement in somatosensory, visual, olfactory, and gustatory processing [20]. Given that we observed significant GMV decline in ventral subnuclei near the lesion, as well as in the intralaminar group, the GMV decrease in the insula may thus be mediated through Wallerian degeneration.

For the ACC, animal studies [21] suggest strong structural connections from the thalamus, particularly from ventral and medial areas. While these connections might exist in humans too, subnuclei data are inchoate and to date primarily show structural connections from the mediodorsal thalamus to the ACC [22]. Indeed, our data suggested some GMV decrease in the mediodorsal thalamus, but this change was not significant. However, the significant correlation we identified between bigger lesion size at 6 months (likely reflecting ablation of adjacent thalamic nuclei) and GMV decline in the ACC supports Wallerian degeneration as a plausible mechanism underlying this change.

Functionally, the insula and ACC are integral components of the salience network, which integrates autonomic and behavioral responses to external stimuli influencing motor regulation, with the thalamus acting as a control hub [18]. Supporting this, Fang and colleagues [23] reported increased functional activity in the salience network among ET patients. Additionally, ET patients often show GMV increases in the frontal lobe and left insula, indicating heightened functional load in these regions [24]. The findings of GMV declines in the left insula and ACC after treatment, might also be attributable to reduced functional demands following tremor improvement, leading to adaptive structural changes in these areas. Diminution of tremor likely reduces the sensory and attentional system requirements, potentially resulting in structural changes as these areas are no longer over-engaged. Taylor and colleagues [25] proposed a resting-state connectivity network between the insula and the cingulate cortex that is involved in skeletomotor body orientation and monitoring. Considering these roles, activity in this network may be reduced due to the absence of tremor which would decrease the demand for motor control and possibly induce intermediate structural reorganization.

Also, the GMV decline in the contralesional middle occipital gyrus might be related to altered sensory input. ET patients showed GMV increases relative to healthy controls in visual areas, suggesting increased demands for visuospatial control in the presence of intention tremor. Moreover, structural and functional changes have been observed in visual areas following tremor reduction due to VIM lesioning or DBS [3,9]. These adaptations may be caused by normalization of the interconnectivity of visual areas due to tremor improvement [26]. A

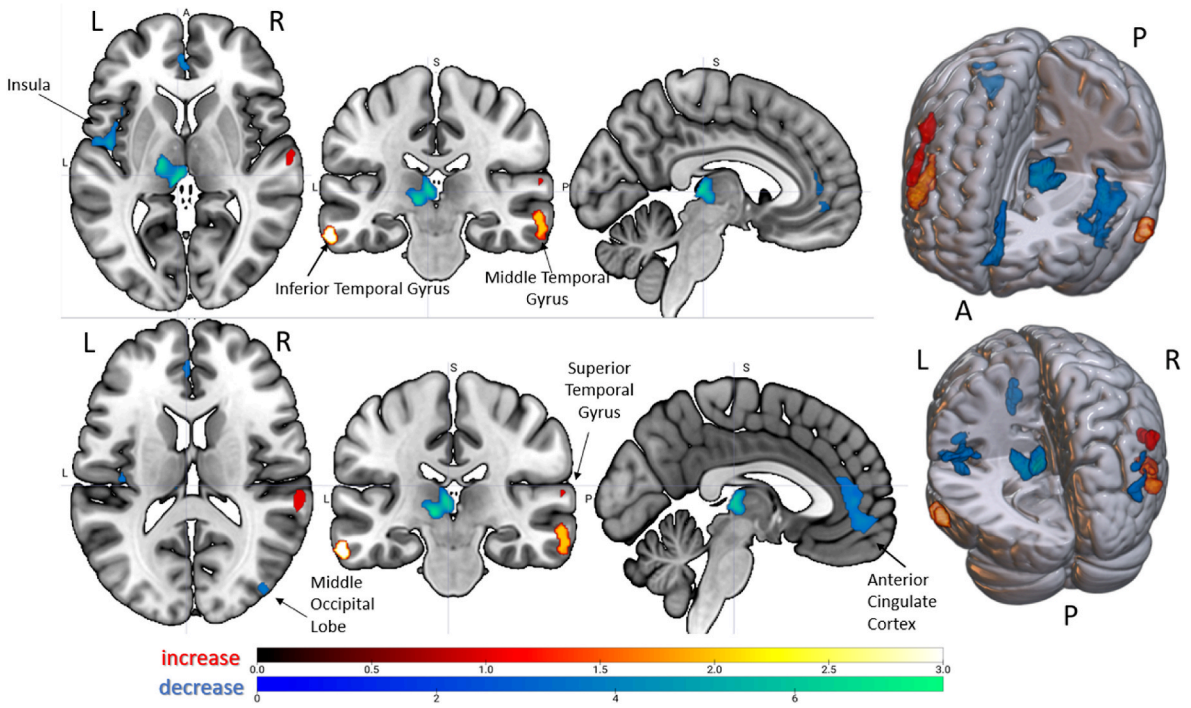

Fig. 3. Whole-brain statistical analysis of gray matter changes: 6 months post MRgFUS versus baseline
Figure Legend. Significant GMV changes in left thalamus, insula/Rolandic operculum, ACC, right middle occipital gyrus (decreases), and temporal gyri (increases). Multiple comparison correction method: FWE cluster-level correction (Decrease: k = 239, Increase: k = 290). Color bars show t-values: green (GMV increase), red/yellow (GMV decrease). (For interpretation of the references to colour in this figure legend, the reader is referred to the Web version of this article.)

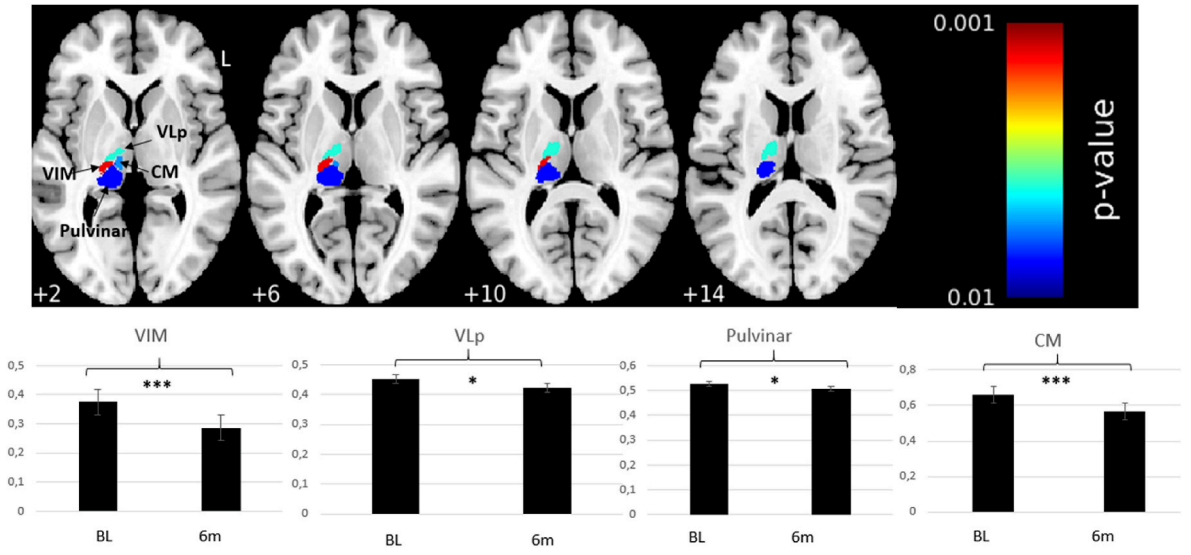

Fig. 4. ROI-based statistical analysis of thalamic subregions: 6 months post MRgFUS versus baseline
Figure legend. Significant GMV reductions at 6m in VIM, CM, VLp, and PV using atlas [15]. Multiple corrections with Bonferroni-Holm (FWE, p = 0.05). Bar charts show GMV at baseline and 6m with standard error (*p = 0.05, ***p < 0.001). (For interpretation of the references to colour in this figure legend, the reader is referred to the Web version of this article.)" after "…***p < 0.001).

significant decrease was observed primarily contralateral to the lesion, but the anatomically connected ipsilateral primary visual cortex also showed a GMV decline at a more lenient threshold.

Our finding of increased GMV in bilateral temporal areas complements observations in untreated ET patients showing decreased GMV in comparison with healthy controls [27]. Previous neuroimaging and electrophysiological recording studies [28] suggested that temporal areas are involved in control of goal-directed movement sequences and sensorimotor coordination. After diminution of tremor, the increase in motor activities involving fine hand movements (e.g., using cutlery, brushing teeth, etc.) may have influenced the demand for sensorimotor control and triggered GMV increases in temporal regions. Supporting this, a DBS connectomics study [29] highlighted the functional relationship between temporal areas, along with visual and motor regions, and tremor improvement. Likewise, our study found a correlation between increased temporal GMV and improved functional abilities in social life and daily living, as measured by the FTM-C and the SF-36. Furthermore, lesion size at 3 days and 6 months was significantly

associated with GMV increases in the left inferior temporal gyrus and right superior temporal gyrus, respectively. A trend-level association between initial lesion size and improved functional abilities on the FTM-C further underscores the potential importance of temporal regions in motor recovery and functional outcomes. It has to be acknowledged, however, that other studies report contrary results, namely increased GMV in the superior and middle temporal areas when comparing ET patients with healthy controls [26].

Generally, our findings likely reflect a combination of mechanisms, including GMV decline in structurally connected areas (insula and ACC) due to Wallerian degeneration, as well as changes in sensory input (occipital and temporal areas) driven by tremor reduction. The latter mechanism may reflect a shift toward a healthier state, as patients regain the ability to perform fine motor tasks (e.g., washing, using cutlery) independently.

It is unlikely that disease progression or general aging could account for the extent of structural decline observed over just six months. Thus, the GMV reductions and increases we report are most plausibly attributed to long-term procedure-related mechanisms rather than a more global or unrelated degenerative process.

While our findings show widespread cortical GMV changes predominantly ipsilateral to the MRgFUS lesion, it is surprising that no significant changes were observed in M1, the primary output region of the VIM as well as other motor areas. Structural changes could have been expected in M1 given that previous data from our group [4] highlighted reductions in streamline counts within the CTCC, particularly in fibers connecting the VIM to ipsilateral M1. Complementing this, task-based fMRI revealed decreased activation in the ipsilateral M1 as well as other motor related areas (e.g. primary somatosensory cortex) following MRgFUS treatment [4]. While therefore structural and functional connectivity changes have been observed and were even associated with tremor control [29], morphometric changes in motor areas have up to this point neither been reported in thalamotomy nor in DBS: Bruno and colleagues [17] found volumetric reductions in the putamen, pallidum, and cerebellar cortex following MRgFUS in ET patients but reported no changes in the motor cortex. Similarly, Bolton et al. [30] examined morphometric normalization after VIM ablation, comparing regional brain structures in patients to those of healthy controls, and observed that M1 did not “normalize” structurally—a phenomenon often discussed in functional connectivity studies [5,30]. These findings suggest that while functional and structural connectivity changes along the VIM-motor pathways support adaptive functions, they do not appear to induce morphometric changes in the terminal motor regions. Further research is needed to explore why these functional adjustments fail to produce measurable GMV alterations. Although this could be depended on study-specific factors of our cohort, such as follow-up intervals or surgical procedure, it could also be explained by compensatory mechanisms occurring and therefore preventing atrophy given that motor areas will be more engaged with the restitution of motor function after tremor reduction.

Similar to the aforementioned morphometric studies [17,30], no association between tremor improvement (FTM-A/B) and GMV changes were found in our study. While this is somewhat unexpected for the thalamic lesion site, the lack of a direct association for regions not involved in tremor generation is more plausible.

Limitations are as follows: This study did not include either healthy or non-treated controls for comparison which could have clarified whether the structural alterations seen in ET patients reflect baseline abnormalities, non-procedural time effects or actual shifts toward a healthier state. Longer follow-up intervals may reveal additional variability with regard to the stability of the tremor improvements, and further neural plasticity also in motor related circuits. Moreover, the inherent heterogeneity in both the clinical presentation of ET patients (e.g., the intensity and type of tremor) and the variability in VIM lesioning locations limits the generalizability of our findings, even with an adequate sample size. Other potential confounding variables like medication use, disease duration or side effects were not controlled for, which could influence the results.

5. Conclusion

Our findings implicate local but also more distributed structural adaptations in areas beyond the CTCT network following unilateral MRgFUS targeting the VIM nucleus. Structural losses could reflect Wallerian degeneration of VIM output neurons and adjacent thalamic subnuclei; or, alternatively, plasticity due to decreased sensory input following tremor improvement. While structural changes were not correlated with tremor decrease, consistent association of GMV increases in temporal areas with improved QoL were reported. In summary, these findings are significant for understanding neuroplasticity following tremor treatment in ET and motivate further research into neural mechanisms of tremor improvement.

CRediT authorship contribution statement

Jonas Krauss: Writing – original draft, Methodology, Investigation, Conceptualization. **Neeraj Upadhyay:** Writing – review & editing, Methodology. **Veronika Purrer:** Writing – review & editing, Data curation. **Valeri Borger:** Writing – review & editing, Data curation. **Marcel Daamen:** Writing – review & editing. **Angelika Maurer:** Writing – review & editing. **Carsten Schmeel:** Writing – review & editing. **Alexander Radbruch:** Writing – review & editing. **Ullrich Wüllner:** Writing – review & editing, Supervision. **Henning Boecker:** Writing – review & editing, Supervision.

Funding agency

The MRgFUS facility was funded by the German Research Foundation (INST 1172/64–1) and the Medical Faculty of Friedrich-Wilhelms-University Bonn.

A.R. receives study support from Bayer Health Care and Guerbet.

U.W. has received consultancy fees from STADA Pharm, Idorsia and Zambon. He has received lecture fees from Abbvie, Bayer, Bial, Roche and Zambon. He has received study support from the DFG, the German Ministry of Research (BMBF), the International Parkinson Fund and the German Parkinson Association (dPV), as well as from the German Center for Neurodegenerative Diseases (DZNE) and the University of Bonn.

H.B. receives grant support from the BONFOR program of the University of Bonn and royalties from Springer.

The other authors declare that they have no known competing financial interests or personal relationships that could have appeared to influence the work reported in this paper.

Ethical standards

The study was approved by the local ethics board of the University Hospital Bonn (No. 314/18), with informed consent from all participants obtained in accordance with the Declaration of Helsinki.

Funding

The MRgFUS facility was funded by the German Research Foundation (INST 1172/64–1).

Declaration of competing interest

The authors declare they have no competing interest.

Acknowledgment

We are grateful to the patients for their participation in this study. Open Access funding enabled and organized by Project DEAL.

Appendix A. Supplementary data

Supplementary data to this article can be found online at https://doi.org/10.1016/j.parkreldis.2025.107318.

References

[1] F. Hopfner, G. Deuschl, Managing essential tremor, Neurotherapeutics 17 (2020) 1603–1621, https://doi.org/10.1007/s13311-020-00899-2.

[2] A.D. Pinto, A.E. Lang, R. Chen, The cerebellothalamocortical pathway in essential tremor, Neurology 60 (2003) 1985–1987, https://doi.org/10.1212/01.wnl.0000065890.75790.29.

[3] C. Kindler, N. Upadhyay, V. Purrer, F.C. Schmeel, V. Borger, L. Scheef, U. Wüllner, H. Boecker, MRgFUS of the nucleus ventralis intermedius in essential tremor modulates functional connectivity within the classical tremor network and beyond, Parkinsonism Relat. Disord. 115 (2023) 105845, https://doi.org/10.1016/j.parkreldis.2023.105845.

[4] E.D.R. Pohl, N. Upadhyay, X. Kobeleva, V. Purrer, A. Maurer, V.C. Keil, C. Kindler, V. Borger, C.C. Pieper, S. Groetz, L. Scheef, J. Maciaczyk, H. Schild, H. Vatter, T. Klockgether, A. Radbruch, U. Attenberger, U. Wüllner, H. Boecker, Coherent structural and functional network changes after thalamic lesions in essential tremor, Mov. Disord. 37 (2022) 1924–1929, https://doi.org/10.1002/mds.29130.

[5] L. Dahmani, Y. Bai, M. Li, J. Ren, L. Shen, J. Ma, H. Li, W. Wei, P. Li, D. Wang, L. Du, W. Cui, H. Liu, M. Wang, Focused ultrasound thalamotomy for tremor treatment impacts the cerebello-thalamo-cortical network, NPJ Parkinsons. Dis. 9 (2023) 90, https://doi.org/10.1038/s41531-023-00543-8.

[6] A.A. Vijayakumari, H.H. Fernandez, B.L. Walter, MRI-based multivariate gray matter volumetric distance for predicting motor symptom progression in Parkinson's disease, Sci. Rep. 13 (2023) 17704, https://doi.org/10.1038/s41598-023-44322-0.

[7] S. Qi, H. Cao, R. Wang, Z. Jian, Y. Bian, J. Yang, Relative increase in cerebellar gray matter in young onset essential tremor: evidence from voxel-based morphometry analysis, J. Clin. Neurosci. 79 (2020) 251–256, https://doi.org/10.1016/j.jocn.2020.07.003.

[8] L. Andrews, S.S. Keller, J. Osman-Farah, A. Macerollo, A structural magnetic resonance imaging review of clinical motor outcomes from deep brain stimulation in movement disorders, Brain Commun 5 (2023) fcad171, https://doi.org/10.1093/braincomms/fcad171.

[9] X. Wang, S. Wang, J. Lin, D. Zhang, H. Lu, Y. Xiong, L. Deng, D. Zhang, X. Bian, J. Zhou, L. Pan, X. Lou, Gray matter alterations in tremor-dominant Parkinson's disease after MRgFUS thalamotomy are correlated with tremor improvement: a pilot study, Quant. Imag. Med. Surg. 13 (2023) 4415–4428, https://doi.org/10.21037/qims-22-1403.

[10] S. Fahn, E. Tolosa, Marín concepcíon, clinical rating scale for tremor, Parkinson's disease and, Mov. Disord. 225 (1988) 234.

[11] J.E. Ware, C.D. Sherbourne, The MOS 36-item short-form health survey (SF-36). I. Conceptual framework and item selection, Med. Care 30 (1992) 473–483.

[12] E.L. Mazerolle, R. Warwaruk-Rogers, P. Romo, T. Sankar, S. Scott, C.P. Rockel, S. Pichardo, D. Martino, Z.H. Kiss, G.B. Pike, Diffusion imaging changes in the treated tract following focused ultrasound thalamotomy for tremor, Neuroimage: Reports 1 (2021) 100010, https://doi.org/10.1016/j.ynirp.2021.100010.

[13] C. Gaser, R. Dahnke, P.M. Thompson, F. Kurth, E. Luders, A.D.N.I. The, CAT: a computational anatomy toolbox for the analysis of structural MRI data, GigaScience 13 (2024), https://doi.org/10.1093/gigascience/giae049.

[14] E.T. Rolls, C.-C. Huang, C.-P. Lin, J. Feng, M. Joliot, Automated anatomical labelling atlas 3, Neuroimage 206 (2020) 116189, https://doi.org/10.1016/j.neuroimage.2019.116189.

[15] M. Saranathan, C. Iglehart, M. Monti, T. Tourdias, B. Rutt, In vivo high-resolution structural MRI-based atlas of human thalamic nuclei, Sci. Data 8 (2021) 275, https://doi.org/10.1038/s41597-021-01062-y.

[16] J.P. Dreier, C.L. Lemale, V. Kola, A. Friedman, K. Schoknecht, Spreading depolarization is not an epiphenomenon but the principal mechanism of the cytotoxic edema in various gray matter structures of the brain during stroke, Neuropharmacology 134 (2018) 189–207, https://doi.org/10.1016/j.neuropharm.2017.09.027.

[17] F. Bruno, E. Tommasino, A. Catalucci, C. Pastorelli, F. Borea, G. Caldarelli, M. Bellini, P. Badini, S. Mancini, C. Santobuono, S. Martino, V. Pagliei, G. Manco, D. Cerone, F. Pistoia, P. Palumbo, F. Arrigoni, E. Di Cesare, C. Marini, A. Barile, A. Splendiani, C. Masciocchi, Evaluation of cerebral volume changes in patients with tremor treated by MRgFUS thalamotomy, Life 13 (2022), https://doi.org/10.3390/life13010016.

[18] W.W. Seeley, The salience network: a neural system for perceiving and responding to homeostatic demands, J. Neurosci. 39 (2019) 9878–9882, https://doi.org/10.1523/JNEUROSCI.1138-17.2019.

[19] A.D.B. Craig, Topographically organized projection to posterior insular cortex from the posterior portion of the ventral medial nucleus in the long-tailed macaque monkey, J. Comp. Neurol. 522 (2014) 36–63, https://doi.org/10.1002/cne.23425.

[20] V.J. Kumar, K. Scheffler, W. Grodd, The structural connectivity mapping of the intralaminar thalamic nuclei, Sci. Rep. 13 (2023) 11938, https://doi.org/10.1038/s41598-023-38967-0.

[21] M. Xue, W.-T. Shi, S.-B. Zhou, Y.-N. Li, F.-Y. Wu, Q.-Y. Chen, R.-H. Liu, Z.-X. Zhou, Y.-X. Zhang, Y.-X. Chen, F. Xu, G.-Q. Bi, X.-H. Li, J.-S. Lu, M. Zhuo, Mapping thalamic-anterior cingulate monosynaptic inputs in adult mice, Mol. Pain 18 (2022) 17448069221087034, https://doi.org/10.1177/17448069221087034.

[22] J.C. Klein, M.F.S. Rushworth, T.E.J. Behrens, C.E. Mackay, A.J. de Crespigny, H. D'Arceuil, H. Johansen-Berg, Topography of connections between human prefrontal cortex and mediodorsal thalamus studied with diffusion tractography, Neuroimage 51 (2010) 555–564, https://doi.org/10.1016/j.neuroimage.2010.02.062.

[23] W. Fang, H. Chen, H. Wang, H. Zhang, M. Liu, M. Puneet, F. Lv, O. Cheng, X. Wang, X. Lu, T. Luo, Multiple resting-state networks are associated with tremors and cognitive features in essential tremor, Mov. Disord. 30 (2015) 1926–1936, https://doi.org/10.1002/mds.26375.

[24] Q. Han, Y. Hou, H. Shang, A voxel-wise meta-analysis of gray matter abnormalities in essential tremor, Front. Neurol. 9 (2018) 495, https://doi.org/10.3389/fneur.2018.00495.

[25] K.S. Taylor, D.A. Seminowicz, K.D. Davis, Two systems of resting state connectivity between the insula and cingulate cortex, Hum. Brain Mapp. 30 (2009) 2731–2745, https://doi.org/10.1002/hbm.20705.

[26] C. Daniels, M. Peller, S. Wolff, K. Alfke, K. Witt, C. Gaser, O. Jansen, H.R. Siebner, G. Deuschl, Voxel-based morphometry shows no decreases in cerebellar gray matter volume in essential tremor, Neurology 67 (2006) 1452–1456, https://doi.org/10.1212/01.wnl.0000240130.94408.99.

[27] E. Cameron, J.P. Dyke, N. Hernandez, E.D. Louis, U. Dydak, Cerebral gray matter volume losses in essential tremor: a case-control study using high resolution tissue probability maps, Parkinsonism Relat. Disord. 51 (2018) 85–90, https://doi.org/10.1016/j.parkreldis.2018.03.008.

[28] S.D. McDougle, S.A. Wilterson, N.B. Turk-Browne, J.A. Taylor, Revisiting the role of the medial temporal lobe in motor learning, J. Cognit. Neurosci. 34 (2022) 532–549, https://doi.org/10.1162/jocn_a_01809.

[29] B. Al-Fatly, S. Ewert, D. Kübler, D. Kroneberg, A. Horn, A.A. Kühn, Connectivity profile of thalamic deep brain stimulation to effectively treat essential tremor, Brain 142 (2019) 3086–3098, https://doi.org/10.1093/brain/awz236.

[30] T.A.W. Bolton, D. van de Ville, J. Régis, T. Witjas, N. Girard, M. Levivier, C. Tuleasca, Dynamic functional changes upon thalamotomy in essential tremor depend on baseline brain morphometry, Sci. Rep. 14 (2024) 2605, https://doi.org/10.1038/s41598-024-52410-y.